



AFRL-RX-WP-TP-2011-4288

**INFLUENCING SOLVENT MISCIBILITY AND AQUEOUS
STABILITY OF OXIDE PASSIVATED ALUMINUM
NANOPARTICLES THROUGH SURFACE
FUNCTIONALIZATION WITH ACRYLIC MONOMERS
(PREPRINT)**

Christopher A. Crouse

UES, Inc.

Christian J. Pierce and Jonathan E. Spowart

Metals Branch

Metals, Ceramics, and NDE Division

JULY 2011

Approved for public release; distribution unlimited.

See additional restrictions described on inside pages

STINFO COPY

**AIR FORCE RESEARCH LABORATORY
MATERIALS AND MANUFACTURING DIRECTORATE
WRIGHT-PATTERSON AIR FORCE BASE, OH 45433-7750
AIR FORCE MATERIEL COMMAND
UNITED STATES AIR FORCE**

REPORT DOCUMENTATION PAGE

Form Approved
OMB No. 0704-0188

The public reporting burden for this collection of information is estimated to average 1 hour per response, including the time for reviewing instructions, searching existing data sources, gathering and maintaining the data needed, and completing and reviewing the collection of information. Send comments regarding this burden estimate or any other aspect of this collection of information, including suggestions for reducing this burden, to Department of Defense, Washington Headquarters Services, Directorate for Information Operations and Reports (0704-0188), 1215 Jefferson Davis Highway, Suite 1204, Arlington, VA 22202-4302. Respondents should be aware that notwithstanding any other provision of law, no person shall be subject to any penalty for failing to comply with a collection of information if it does not display a currently valid OMB control number. **PLEASE DO NOT RETURN YOUR FORM TO THE ABOVE ADDRESS.**

1. REPORT DATE (DD-MM-YY) July 2011			2. REPORT TYPE Journal Article Preprint		3. DATES COVERED (From - To) 01 July 2011 – 01 July 2011	
4. TITLE AND SUBTITLE INFLUENCING SOLVENT MISCIBILITY AND AQUEOUS STABILITY OF OXIDE PASSIVATED ALUMINUM NANOPARTICLES THROUGH SURFACE FUNCTIONALIZATION WITH ACRYLIC MONOMERS (PREPRINT)						5a. CONTRACT NUMBER In-house
						5b. GRANT NUMBER
						5c. PROGRAM ELEMENT NUMBER 62102F
6. AUTHOR(S) Christopher A. Crouse (UES, Inc.) Christian J. Pierce and Jonathan E. Spowart (AFRL/RXLM)						5d. PROJECT NUMBER 4347
						5e. TASK NUMBER 20
						5f. WORK UNIT NUMBER BP108102
7. PERFORMING ORGANIZATION NAME(S) AND ADDRESS(ES) UES, Inc. Dayton, OH 45432						8. PERFORMING ORGANIZATION REPORT NUMBER AFRL-RX-WP-TP-2011-4288
Metals Branch (AFRL/RXLM) Metals, Ceramics, and NDE Division Air Force Research Laboratory, Materials and Manufacturing Directorate Wright-Patterson Air Force Base, OH 45433-7750 Air Force Materiel Command, United States Air Force						
9. SPONSORING/MONITORING AGENCY NAME(S) AND ADDRESS(ES) Air Force Research Laboratory Materials and Manufacturing Directorate Wright-Patterson Air Force Base, OH 45433-7750 Air Force Materiel Command United States Air Force						10. SPONSORING/MONITORING AGENCY ACRONYM(S) AFRL/RXLM
						11. SPONSORING/MONITORING AGENCY REPORT NUMBER(S) AFRL-RX-WP-TP-2011-4288
12. DISTRIBUTION/AVAILABILITY STATEMENT Approved for public release; distribution unlimited.						
13. SUPPLEMENTARY NOTES PAO Case Number: 88ABW 2010-2298; Clearance Date: 28 Apr 2010. Document contains color. Journal article submitted to <i>ACS Applied Materials & Interfaces</i> .						
14. ABSTRACT With increasing interest in the development of new composite systems for a variety of applications which require easily processible materials and adequate structural properties with high energy densities, we have pursued the chemical functionalization of oxide passivated aluminum nanoparticles (nAl) using three acrylic monomers, 3-(trimethoxysilyl)propyl methacrylate (MPS), 2-carboxyethyl acrylate (CEA) and phosphoric acid 2-hydroxyethyl methacrylate ester (PAM), to provide chemical compatibility within various solvent and polymeric systems. FTIR and XPS suggest that attachment of MPS and PAM monomers occurs through the formation of bonds directly to the passivated oxide surface upon reaction with surface hydroxyls, whereas CEA monomers interact through the formation of ionic carboxylate binding to aluminum atoms within the oxide. The coated particles demonstrate enhanced miscibility in common organic solvents and monomers while MPS and PAM coatings are additionally shown to inhibit oxidation of the aluminum particles when exposed to aqueous environments at room temperature while PAM coatings are stable at even at elevated temperature.						
15. SUBJECT TERMS aluminum, nanoparticles, functionalization, monomer, composites, oxidation						
16. SECURITY CLASSIFICATION OF: a. REPORT Unclassified			17. LIMITATION OF ABSTRACT: SAR	18. NUMBER OF PAGES 36	19a. NAME OF RESPONSIBLE PERSON (Monitor) Jonathan E. Spowart 19b. TELEPHONE NUMBER (Include Area Code) N/A	

Influencing solvent miscibility and aqueous stability of oxide passivated aluminum nanoparticles through surface functionalization with acrylic monomers

Christopher A. Crouse,^{a,b*} Christian J. Pierce^a and Jonathan E. Spowart^a

^a *Air Force Research Laboratory, Materials and Manufacturing Directorate, Wright-Patterson Air Force Base, OH 45433, USA*

^b *UES, Inc., Dayton, OH 45432, USA*

*Corresponding author: christopher.crouse@wpafb.af.mil

Abstract

With increasing interest in the development of new composite systems for a variety of applications which require easily processible materials and adequate structural properties with high energy densities, we have pursued the chemical functionalization of oxide passivated aluminum nanoparticles (nAl) using three acrylic monomers, 3-(trimethoxysilyl)propyl methacrylate (MPS), 2-carboxyethyl acrylate (CEA) and phosphoric acid 2-hydroxyethyl methacrylate ester (PAM), to provide chemical compatibility within various solvent and polymeric systems. FTIR and XPS suggest that attachment of MPS and PAM monomers occurs through the formation of bonds directly to the passivated oxide surface upon reaction with surface hydroxyls, whereas CEA monomers interact through the formation of ionic carboxylate binding to aluminum atoms within the oxide. The coated particles demonstrate enhanced miscibility in common organic solvents and monomers while MPS and PAM coatings are additionally shown to inhibit oxidation of the aluminum particles when exposed to aqueous environments at room temperature while PAM coatings are stable at even at elevated temperature.

Keywords: aluminum, nanoparticles, functionalization, monomer, composites, oxidation

Introduction

Micron-scale aluminum powders (micron-Al) are commonly used as additives and/or fuel in various applications requiring high energy output (propulsion, explosives and pyrotechnics). The increase in specific surface area (SSA) that is gained by replacing micron-scale aluminum powders with aluminum nanopowders (nAl) in energetic materials has been well documented to have a profound impact on the overall reactivity of the material. Nanopowder formulations are capable of demonstrating reaction rates that are orders of magnitude faster than those observed for conventional formulations prepared with

micron-sized powders, additionally these materials also allow for lower ignition times and higher energy output.^{1,2,3,4,5} This dramatic enhancement in reactivity, owing to the high SSA of nAl, has initiated global research efforts focused on replacing micron-Al with nAl in modern energetic formulations, in addition to the exploration and development of new formulations based solely upon nAl as the primary fuel.^{6,7} Although an increase in SSA is welcomed from the standpoint of material reactivity it can also be detrimental from the perspective of materials processing and preparation. In general, nanoparticles possess a higher surface energy than larger particles and hence are more susceptible to particle aggregation (to minimize the free energy).⁸ Additionally, the high surface area associated with nanopowders can lead to dramatic increases in viscosity when combined with solvent or polymeric binder during composite preparation and processing.⁹ Furthermore, as particle size decreases and SSA increases the relative volume of the passivated oxide layer is no longer negligible and can account for a significant percentage of mass.⁴ Most commercial nAl powders prepared with a passivated oxide coating typically exhibit 70-85% active (metallic) aluminum content by mass, the remaining mass is due to the oxide shell on the particles which is effectively inert material and does not directly participate in the combustion process. Although the passivated oxide layer stabilizes the particles by limiting their pyrophoric nature and providing a protective barrier to further oxidation, under prolonged exposure to air or moisture oxidation can still occur.¹⁰ Alternative passivation techniques and/or secondary coatings which are designed to further increase the oxidation resistance of the particles or limit the oxide thickness, could potentially expand processing capabilities for these materials.^{9,10,11,12,13,14} Additionally, coatings which effectively stabilize the particles under oxidative environments, such as aqueous dispersions, would also be beneficial for applications which utilize water as the primary oxidizing agent.

Chemical functionalization of the nanoparticle surface is a common technique used in the preparation of nanoparticle/polymer composites to minimize particle aggregation by altering the chemistry of the nanoparticle surface with an organic corona that is compatible with the polymer. The ligands selected to bridge the gap between the nanoparticle and the polymer matrix are often multifunctional, displaying both a reactive moiety capable of chemically or physically interacting with the nanoparticle surface and an organic component that affords favorable interaction with the polymer matrix.¹⁵ The particle architecture for nAl consists of a crystalline metallic aluminum core stabilized by a thin (2-6 nm) amorphous aluminum oxide shell on the exterior of the particle. Altering the surface chemistry therefore requires ligands which are capable of chemically (or physically) interacting with the amorphous aluminum oxide surface. Under standard atmospheric conditions, the amorphous oxide layer can become partially hydroxylated,¹⁶ thereby providing a route towards chemical

functionalization.^{17,18,19,20} Several groups have explored the formation of self-assembled monolayers (SAMs) on the oxide surface of bulk aluminum and other metal oxide surfaces utilizing the condensation of carboxylic acids to surface bound hydroxyls.^{17,19,20,21} Successful functionalization of alumina surfaces with silanes^{22,23,24} and phosphoric acids^{25,26} has also been reported. Similar approaches have also been explored and applied to incorporate alumina nanoparticles into polymer composites,^{27,28} yet only limited examples exist in which the functionalization of nAl with organic ligands through modification of the thin passivated oxide layer has been investigated. For example, the work of Liu et al. has demonstrated that organosilanes can be used to effectively alter the surface chemistry of flaky aluminum particles to promote dispersion in poly(methyl methacrylate) for pigment applications.^{29,30}

Developing new nAl composite systems that possess adequate structural properties while also maintaining the energetic properties necessary to meet a desired application often requires the use of very large particle loadings, therefore chemical interaction between the particles and the matrix which they are imbedded is desired to improve the mechanical properties of the material. To this end we have pursued the chemical functionalization of commercially available aluminum nanoparticles using three acrylic monomers, 3-methacryloxypropyltrimethoxysilane (MPS), 2-carboxyethyl acrylate (CEA) and phosphonic acid 2-hydroxyethyl methacrylate ester (PAM), to afford compatibility within various polymeric systems. Detailed characterization of these novel coatings along with their impact on the reactivity of the nAl powder is presented.

Materials and Methods

Chemicals

Aluminum powder (<50 nm spherical, 18 nm mean particle size, Lot # C11T058) was purchased from Alfa Aesar and stored under argon in a glove box ($O_2 \leq 1$ ppm; dew point = -80 °C) prior to use. 3-methacryloxypropyltrimethoxysilane (MPS), 2-carboxyethylacrylate (CEA), phosphoric acid 2-hydroxyethyl methacrylate ester (PAM), methyl methacrylate (MMA), cyclohexanone, 2,2'-Azobis(2-methylpropionitrile) (AIBN) and hydroquinone were purchased from Aldrich and used as received unless otherwise noted. Toluene and acetonitrile were obtained from Fisher Scientific and were dried by refluxing over CaH_2 followed by distillation prior to use. MMA and cyclohexanone were also dried over CaH_2 and distilled prior to use. AIBN was recrystallized from acetone prior to use.

Table 1 Reaction conditions for monomer functionalization of nAl

Sample	nAl (g)	Monomer (g)			Solvent (mL)	
		MPS	CEA	PAM	Toluene	Acetonitrile
MPS-co-nAl	1.0	2.48	--	--	100	--
CEA-co-nAl	1.0	--	1.44	--	100	--
PAM-co-nAl	1.0	--	--	2.38 ^a	--	100

^a The average molecular weight for PAM was calculated to be 238.14 g.mol⁻¹ based upon a 25% diester content.

Monomer functionalization of nAl

The specific reagent concentrations used to prepare the monomer functionalized particles are displayed in Table 1. A typical reaction for the functionalization of nAl with CEA to yield CEA-co-nAl was performed as follows. A 250-mL, four-necked round bottom flask, fitted with an overhead stirrer, two rubber septa, and a glass stopper was charged with nAl powder (1.0 g, 37 mmol) and hydroquinone (0.050 g, 0.45 mmol), which was added as a radical scavenger to prevent polymerization during the reaction. A nitrogen atmosphere was established and maintained in the reaction vessel. In a separate 100-mL, single-neck round bottom flask, CEA (1.48 g, 10.0 mmol) was dissolved into 100-mL of dry toluene under nitrogen. The monomer solution was transferred via canula to the reaction vessel and stirring (250 rpm) was started. The reaction vessel was then submerged into an external oil bath held at 60 °C. The reaction was allowed to progress for 16 hours with samples removed at specific time intervals to monitor the reaction progress. The functionalized particles were isolated by vacuum filtration over a 0.2 µm PTFE membrane and washed with toluene and acetone to remove physisorbed monomer. The filtered product was then dried in a vacuum desiccator to remove residual solvent prior to analysis. Surface functionalization of nAl with MPS and with PAM monomers to yield MPS-co-nAl and PAM-co-nAl, respectively, was performed using the same procedure described above with the exception that CH₃CN was used as the solvent for PAM functionalization as noted in Table 1.

Synthesis of poly(2-carboxyethylacrylate)

A three-neck round bottom flask, fitted with rubber septa and a magnetic stirbar, was charged with CEA (10.0 g, 0.069 mol) then sealed and placed under a nitrogen atmosphere. AIBN (0.100 g, 0.61 mmol) was dissolved into dry toluene (25 mL) and added to the reaction vessel via the use of a cannula. The vessel was then immersed into an oil bath at 75 °C and held for 2 hours with continuous stirring. Upon reaction the solution increased in viscosity and eventually formed a translucent gel as the polymer precipitated.

Heat was removed and the reaction was allowed to cool. The polymer was isolated by vacuum filtration and washed with acetone to remove residual monomer and solvent. The final product was dried open to air and then placed into a vacuum desiccator overnight to remove residual solvent. Yield: 9.45 g (94.5%)

Synthesis of poly(phosphoric acid 2-hydroxyethyl methacrylate ester)

A three neck round bottom flask, fitted with rubber septa and a magnetic stir bar, was charged with PAM (7.0 g, 0.029 mol) then sealed and placed under a nitrogen atmosphere. AIBN (0.070 g, 0.43 mmol) was dissolved into dry cyclohexanone (25 mL) and added to the reaction vessel via the use of a cannula. The vessel was then immersed into an oil bath at 75 °C and held for 2 hours with continuous stirring. Upon reaction the solution experienced an increase in viscosity and eventually formed a white gel as the polymer precipitated. Heat was removed and the reaction was allowed to cool. The polymer was isolated by vacuum filtration and transferred into a Soxhlet extractor where it was washed with acetone for 16 hours to remove residual monomer and solvent. The polymer was then dried open to air and then placed into a vacuum desiccator overnight to remove residual solvent. Yield: 6.44 g (92.0%)

Characterization

Thermogravimetric analysis (TGA) was performed on a TA Instruments SDT Q600 dual TGA/DTA. Samples (5 to 20 mg) were placed into a tared alumina crucible with an empty alumina crucible serving as the reference. All data were collected in dynamic mode under flowing argon (100 mL/min) from room temperature up to 600 °C at a rate of 10 °C/min.

Fourier Transform Infrared (FTIR) absorption spectra were obtained from dry powders on a Perkin-Elmer L100 FTIR absorption spectrophotometer equipped with an attenuated total reflectance (ATR) sample attachment.

High resolution transmission electron microscopy (HR-TEM) images were acquired on a FEI Titan HR-TEM with a CS corrector at an operating voltage of 300 keV. Samples were prepared by drop-drying a dilute solution of functionalized particles suspended in acetone or hexanes onto a 200-mesh copper grid coated with a holey carbon film (Ted Pella, Inc.).

X-ray photoelectron spectroscopy (XPS) was performed on a Surface Science Instruments M-Probe using monochromatic Al K_{α} X-rays (energy 1486.6 eV). XPS samples were prepared by casting a drop of functionalized particles suspended in acetone or hexanes onto a 10 mm x 10 mm silicon wafer coated with a native oxide and allowing the solvent to evaporate leaving behind a thin film. CasaXPS software was used for curve fitting and interpretation of XPS signals.

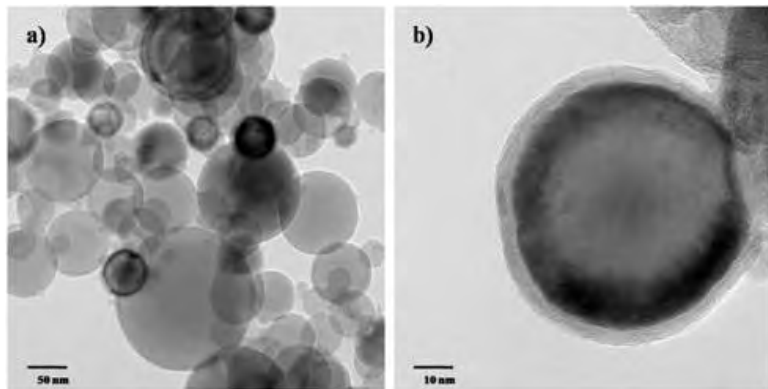
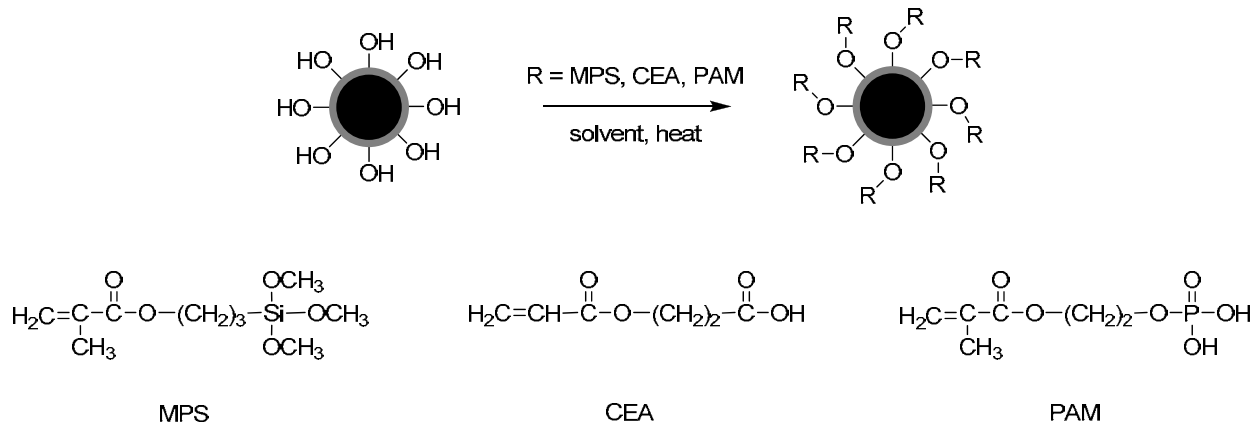


Fig. 1 TEM images of a) commercial nAl obtained from Alfa Aesar and b) a single particle to show the typical particle architecture consisting of an aluminum core and amorphous aluminum oxide passivation layer.

Results and Discussion

The nAl particles used in this study exhibit a core-shell type structure with an amorphous oxide passivation layer (*ca.* 4 nm) and a crystalline metallic aluminum core, Fig. 1. Particle size distribution for the neat material was broad, displaying a mean size of 80 ± 47 nm as determined through TEM analysis. Aggregation and the presence of fused oxide layers between adjacent particles were also observed in the raw material. The monomeric ligands used in this study, MPS, CEA, and PAM, were selected due to their respective silane, carboxylic acid, and phosphoric acid moieties which are known to react with the surface hydroxyls present on aluminum oxide, thereby covalently anchoring the monomers to the oxide surface,^{17,19,20,21,22,23,24,25,26} as illustrated in Scheme 1. Additionally, the acrylic portion of each ligands should provide the opportunity to directly incorporate the particles into nanocomposite systems.



Scheme 1 Illustration demonstrating monomer functionalization of oxide passivated nAl and the chemical structures for the described monomeric ligands.

Thermogravimetric analysis (TGA)

TGA was used to monitor the reaction efficiency through measuring the mass loss due to the decomposition of the organic component within each powder. The organic should primarily be comprised of monomer, either physisorbed, bound, or in polymer form, on the particle surface. An argon atmosphere was maintained for all TGA analyses to prevent oxidation of metallic aluminum. Fig. 2 contains an overlay of the TGA curves acquired for the three monomer functionalized powders after 16 hours of reaction time. As a measure of the reaction efficiency, Eq. 1 was used to calculate an approximate surface density (molecules/nm²) for each monomeric ligand.

$$Grafting density = \left(\frac{wt\%}{100-wt\%} \right) \frac{6.02 \times 10^{23}}{MW \times SSA} \quad (1)$$

Wt% is the weight percentage due to loss of ligand as determined from TGA analysis and MW is the molecular weight for the ligand of interest. SSA for the neat Alfa Aesar nAl particles was estimated to be $33.1 \times 10^{18} \text{ nm}^2/\text{g}$ based upon particle size distribution data obtained from TEM analysis. This estimated SSA value compares favorably with nAl powders available from other manufacturers.³¹ The grafting densities calculated for the three ligands are displayed in Table 2.

Table 2 Monomer grafting densities calculated from TGA mass loss

Sample	MW_{monomer} (g/mol)	Mass loss (wt% _{TGA})	Grafting Density (molecules/nm ²)
MPS- <i>co</i> -nAl	248.35	4.5	3.3
CEA- <i>co</i> -nAl	144.13	23	37
PAM- <i>co</i> -nAl	238.14 ^a	29	31

^a The average molecular weight for PAM was calculated to be 238.14 g.mol⁻¹ based upon a 25% diester content.

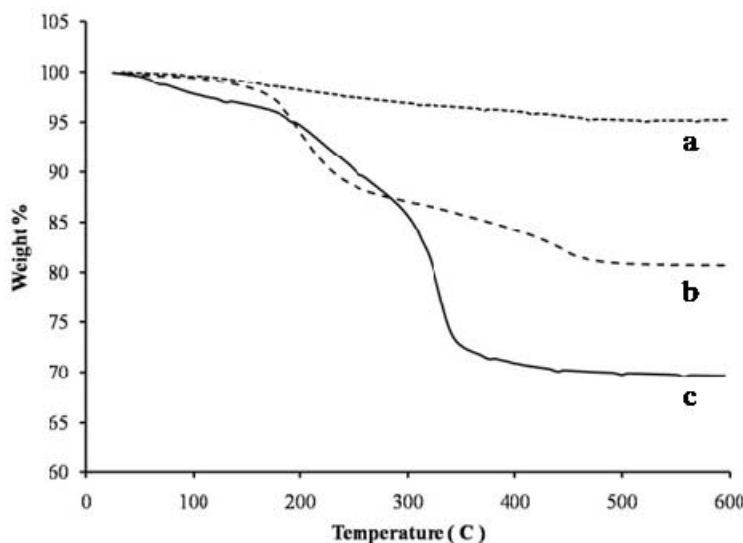


Fig. 2 Overlay of TGA curves for a) MPS-*co*-nAl, b) CEA-*co*-nAl and c) PAM-*co*-nAl

Decomposition of MPS-*co*-nAl occurs gradually with no significant loss below 100 °C. The loss between 100 – 500 °C accounts for *ca.* 4.5% of the sample weight with the primary loss occurring above 200 °C. This implies that the organic layer is relatively thermally stable signifying that MPS is not simply physisorbed but instead interacts with the particle surface likely through the formation of covalent bonds to the oxide. Previous studies which explored the formation of SAMs from alkanesiloxanes on SiO₂/Si surfaces specify a grafting (packing) density equal to 4-5 molecules/nm² is obtained for the monolayers.³² Since the hydroxyl density on amorphous aluminum oxide is reported to be 3 – 15 nm⁻², approximately 1-3 times greater than SiO₂/Si surfaces,³³ a monolayer of monomeric ligands employed in our study would experience a density similar to, or slightly greater than, that reported for alkylsiloxanes on SiO₂ if differences between the organic components are assumed to have a negligible impact on

packing efficiency. After applying this assumption, a grafting density of 3.3 molecules/nm² would suggest that MPS reacts to form near monolayer coating on the particle surface after 16 hours of reaction time.

The decomposition of CEA-*co*-nAl displayed a three-stage loss accounting for *ca.* 23% of the sample weight. This appreciably larger loss suggests that a large percentage of the ligand on the surface of the particle is either physisorbed or has undergone polymerization. The minor loss between 100 – 200 °C is due to evaporation of physisorbed monomer while the more significant loss between 200 – 320 °C is believed to correspond to two separate events which occur simultaneously. First, the decomposition of any CEA that was covalently bound to the oxide surface would be expected to occur during this temperature range. Second, if any polymerization did occur during the course of the reaction then decomposition and depolymerization of the polymer could also occur over this temperature range. Acrylic polymers, when produced by free-radical polymerization, undergo decomposition and depolymerization in multiple stages if they contain any unsaturated double bonds at the chain ends or head-to-head bonding present in the polymer backbone.^{34,35} Furthermore, since the CEA monomers are terminated with a carboxylic acid on the pendant group, adjacent monomer units could also react through condensation yielding an anhydride and eliminating water as is observed in the decomposition of poly(acrylic acid) and poly(methacrylic acid).^{36,37} If no polymer or adsorbed monomer were present then dehydration to form an anhydride would not be possible since the carboxylic acid portion of the monomer would be bound to the oxide surface and not free to react with adjacent monomers.

To confirm if polymer was present in the sample, we prepared poly(2-carboxyethylacrylate) from the CEA monomer using AIBN as an initiator. Decomposition of the poly(2-carboxyethylacrylate) (Fig. S1) demonstrates a multi-stage weight loss curve similar to that observed for CEA-*co*-nAl. The initial loss between 200 – 300 °C indicates that unsaturated end groups are likely present; condensation of carboxylic acids to form anhydrides could also occur in this temperature range. The second loss, 350 – 450 °C, occurs due to decomposition and depolymerization from the more stable saturated chain ends. The similarities between decomposition of CEA-*co*-nAl powder and poly(2-carboxyethylacrylate) leads us to believe that CEA exists in the form of both grafted monomer *and* polymer on the nAl surface. It is the presence of polymer that is responsible for the high grafting density that was observed for this ligand.

The mass loss due to decomposition of ligand in PAM-*co*-nAl accounted for *ca.* 29% of the sample weight. The initial loss, 50 – 250 °C, is due to physisorbed (unbound) monomer. This was followed by a second loss, 250 – 350 °C, attributed to monomer that is covalently anchored to the oxide surface. Since the calculated graphing density for PAM-*co*-nAl is higher than would be expected for a

monolayer coating of the ligand it is possible, as in the case of CEA-*co*-nAl, that polymerization may have occurred during the course of the reaction. To confirm if polymer was present in the sample, we prepared poly(phosphoric acid 2-hydroxyethyl methacrylate ester) from the PAM monomer using AIBN as an initiator in the absence of nAl. An overlay comparing the decomposition of PAM-*co*-nAl with both PAM monomer and poly(phosphoric acid 2-hydroxyethyl methacrylate ester) (Fig. S2) indicates that the decomposition of PAM-*co*-nAl is very different from poly(phosphoric acid 2-hydroxyethyl methacrylate ester). Therefore, it is unlikely PAM exists in polymer form on the particle surface but could still exist in the form of a strongly adhered multilayer thus leading to the larger than anticipated surface grafting density.

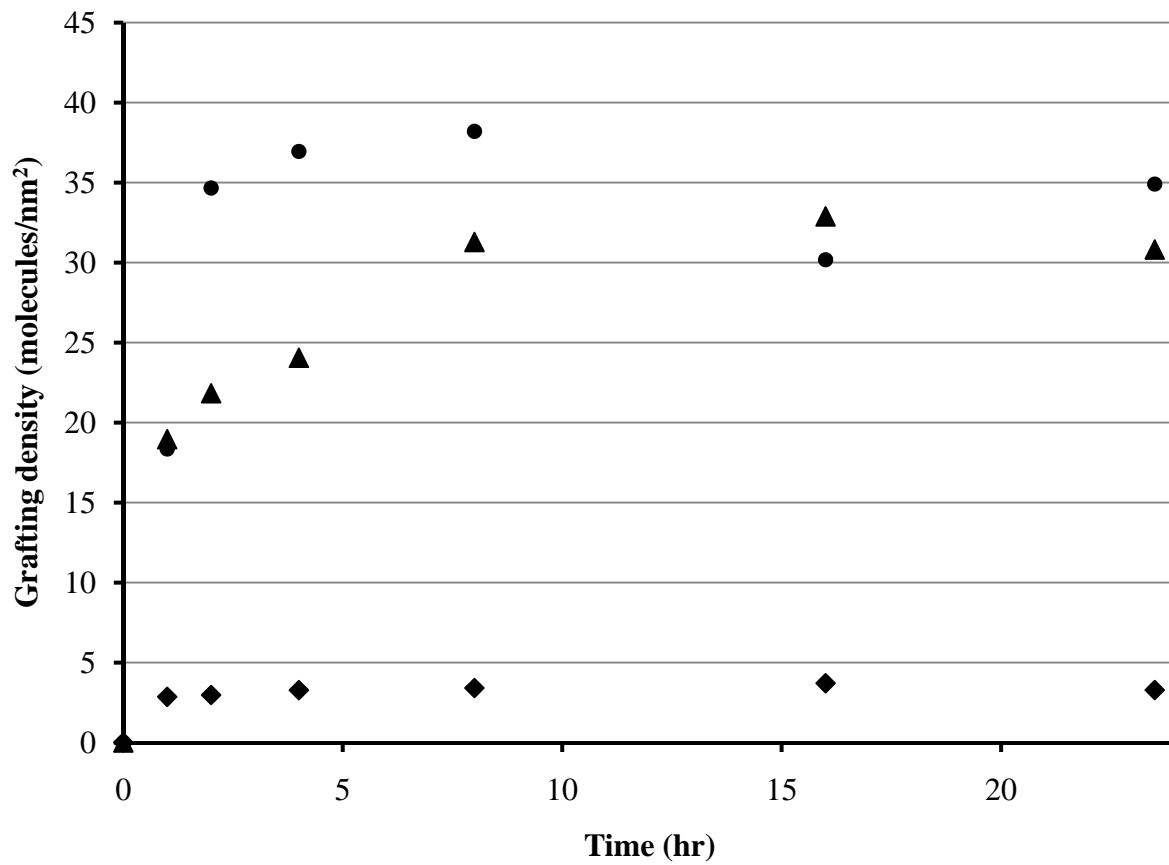


Fig. 3 Time dependence on functionalization grafting density for a) MPS-*co*-nAl, b) CEA-*co*-nAl and c) PAM-*co*-nAl.

Following our initial TGA investigation a time-dependence study was performed to monitor reaction progression and determine the time required to achieve complete functionalization for each monomer. Reactions were performed using the procedure described in the Experimental section with sample aliquots being removed from the reaction vessel at specified time intervals of 0.5, 1, 1.5, 2, 4, 8, and 16 hours. TGA analysis was again used to determine the mass loss attributed to the respective ligands in each of the functionalized samples. These values were then converted to a grafting density using Eq. 1 and plotted with respect to the total reaction time (Fig. 3).

The data presented in Fig. 3 indicate that a maximum grafting density is achieved, irregardless of the monomeric ligand, in less than 8 hours at 60 °C. Previous studies which explored the grafting of MPS onto larger, flaky aluminum particles for pigment applications reported that reaction times on the order of 24 hours were needed to achieve complete functionalization at room temperature.²⁹ It was also shown that an increase in temperature resulted in more efficient grafting for MPS on flaky aluminum,²⁹ which was the basis for the use of elevated temperatures in our functionalization reactions. Our results, however, demonstrate that much shorter reaction times were necessary to achieve a similar degree of functionalization. This observed increase in the reaction rate for MPS functionalization on nAl is likely attributed to the dramatic increase in overall SSA associated with the nAl particles. The slightly higher temperatures present in our reaction condition would also be expected to accelerate the functionalization process.

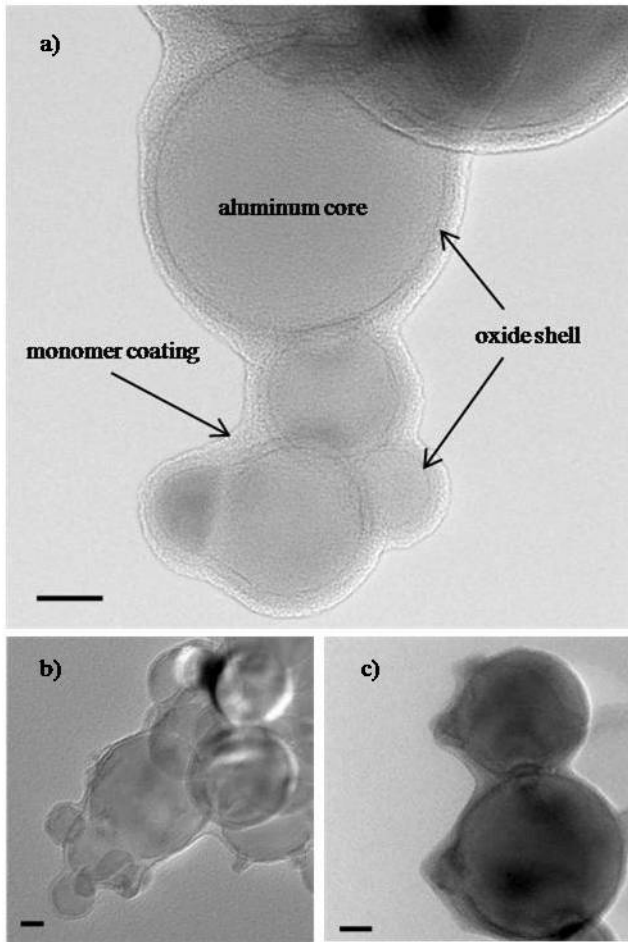


Fig. 4 TEM images of monomer coatings on nAl. a) MPS-*co*-nAl, b) CEA-*co*-nAl and c) PAM-*co*-nAl. Scale bars are 20 nm.

Surface analysis

HR-TEM images of the functionalized powders were able to provide visual evidence of the monomer coatings on the oxide surface for all three systems. The images, displayed in Fig. 4, show a continuous organic coating present on each of the functionalized powders. Despite functionalization, the TEM images demonstrate that the particles remain aggregated indicating that functionalization, though effective at altering the chemistry of the particle surface, has little effect on breaking up the large aggregates of particles. Though functionalization is a technique commonly used to prevent or minimize aggregation in other particle systems, the mild conditions which were utilized in this study, e.g. simple stirring as opposed to high power sonication or high-shear mixing, would not be expected to break up particles which are strongly adhered to each other. Additionally, this observation can possibly be explained by the presence of fused layers oxides which are formed during the passivation process

and result in multiple particles sharing a common oxide layer thereby permanently linking the particles together.

FTIR analysis of the functionalized powders was performed to confirm the addition of the respective ligands to the nAl surface and to provide insight into their specific bonding interactions. Fig. 4 contains FTIR spectra which were obtained for each of the dry functionalized powders and the neat (unfunctionalized) nAl powder. The spectrum for neat nAl was rather featureless aside from the presence of a broad peak at 3305 cm^{-1} which indicates the presence of hydroxyls on the amorphous oxide surface. Additionally, an intense, yet broad, peak which appears at low wavenumbers ($900 - 750\text{ cm}^{-1}$) confirms the presence of Al-O bonds in the amorphous oxide layer.³⁸ The spectra acquired for the ligand functionalized nAl powders were clearly different from that of the neat powder each displaying peaks attributed to their respective monomeric ligand that were not present in the neat nAl powder. A summary of the characteristic peaks and their assignments for each of the functionalized powders and the unfunctionalized nAl is presented in Table 2.

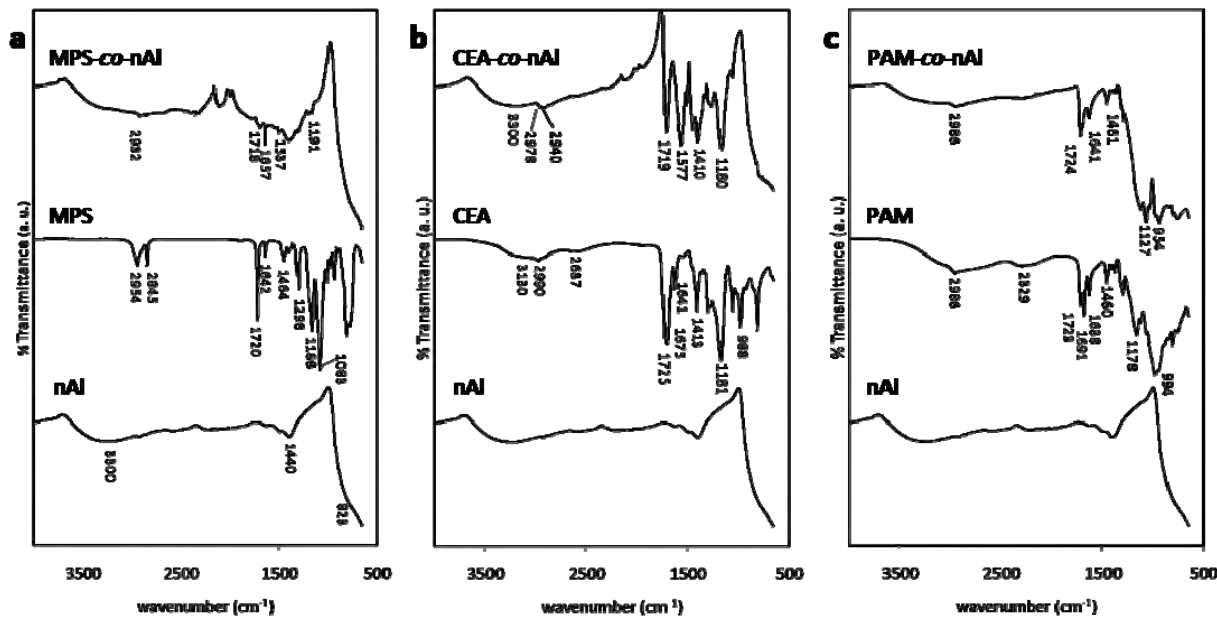


Fig. 5 Overlays of FTIR spectra recorded for a) MPS-*co*-nAl, b) CEA-*co*-nAl and c) PAM-*co*-nAl in comparison to the respective neat monomers and nAl.

Table 3 FTIR peak positions and assignments for functionalized nAl powders

Sample	Wavenumber (cm ⁻¹)	Assignment
nAl	3330 (br)	-O-H stretch
	900-750 (br)	Al-O stretch
MPS- <i>co</i> -nAl	2932	aliphatic C-H stretch
	1718	C=O in unsaturated ester
	1657	C=C stretch
	1191	C-O-C ester antisym stretch
CEA- <i>co</i> -nAl	3300 (br)	-O-H stretch
	2978, 2940	aliphatic C-H stretch
	1719	C=O in unsaturated ester
	1577	-COO ⁻ antisym stretch
	1180	C-O-C ester antisym stretch
PAM- <i>co</i> -nAl	2986	aliphatic C-H stretch
	1724	C=O in unsaturated ester
	1641	C=C stretch
	1461	CH ₂ scissor vibration
	954	P-O-C antisym stretch

The absorptions observed for MPS-*co*-nAl powder were much less intense than those observed for the other functionalized powders due to the low organic content present on the oxide surface. However weak, the presence of peaks due to aliphatic C-H stretching, C=O and C-O-C in the methacrylate ester, and C=C confirm the addition of the ligand on the surface. The presence of a broad shoulder centered at 3300 cm⁻¹ suggests that some -OH groups on the oxide surface remain unreacted. The absence of a strong peak between 1100-1000 wavenumbers, due to Si-O-Si stretching, suggests it is unlikely that MPS has undergone reaction with itself during the functionalization process to form a significant siloxane network at the particle surface as was observed in previous studies with

organosilanes on alumina surfaces.³⁹ This is most likely due to the dry environment utilized in our reaction conditions as these reactions are typically catalyzed by the presence of moisture.

Similar observations were made in the spectrum of the CEA-*co*-nAl. Weak peaks arising from aliphatic C-H stretching accompanied by strong peaks due to absorptions from C=O stretching confirm the addition of CEA. The intense peak at 1574 cm⁻¹ was assigned to COO^- suggesting that the majority of the monomer is attached to the oxide surface through an ionic $\text{COO}^- \text{Al}^+$ interaction. Other researchers studying octadecanoic acid monolayers on sapphire substrates have attributed this peak to bidentate interactions of the carboxylate with individual aluminum atoms at the oxide surface.¹⁹ The lack of a an absorption from C=C stretching at 1640 cm⁻¹ can possibly be explained by the intensity of the COO^- stretch overlapping with the C=C stretching region. Additionally, the C=C peak would also be absent if polymerization had occurred during the course of the reaction, as was suggested by the TGA data, since the unsaturated C=C would become saturated after polymerization.

The spectrum for PAM-*co*-nAl demonstrates absorptions due to aliphatic C-H stretching as well as C=O and C=C stretching. Additionally, the peak appearing at 954 cm⁻¹ suggests that P-O-C stretching is also present. As these absorptions are absent from the neat nAl powder, their presence confirms the attachment of PAM to the oxide surface.

XPS spectra were acquired in parallel to FTIR data collection. Survey spectra (Fig. S3), probing binding energies from 0 – 1000 eV (0 – 600 eV are displayed), were obtained for the neat nAl powder and the three dry functionalized powder samples to confirm elemental composition. All of the samples, including the unfunctionalized nAl powder, displayed peaks corresponding to O1s (532 eV), C1s (285 eV), Al2p (73 eV) and Al2s (120 eV) peaks. The presence of a C1s signal in the nAl spectra arises from background carbon in the chamber or possible contamination due to adsorbed organics. Detection of silicon, Si2s (99 eV), and phosphorous, P2p (130 eV) and P2s (190 eV), in the MPS-*co*-nAl and PAM-*co*-nAl powders, respectively, confirmed the presence of both monomers on the particles as these elements were not present in the neat powder but come from the silane and phosphoric acid moieties in the respective monomer . Due to background carbon present in the system, and possible carbon contamination in the neat nAl, the survey spectrum for CEA-*co*-nAl was not sufficient to confirm the addition of carbon (or oxygen), however, an increase in the O/Al and C/Al ratios (O/Al = 7.0 and C/Al = 3.4) from those in the neat nAl powder (O/Al = 5.0 and C/Al = 1.2), along with the TGA and FTIR data, confirms that the functionalization was successful.

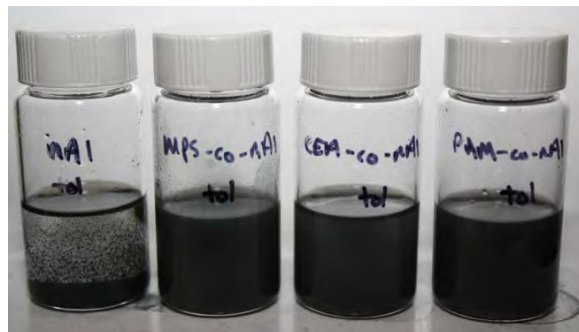
Solvent miscibility and oxidation resistance

The formation of bonds between the the respective silane, carboxylic acid, and phosphoric acid portions of each ligand with the hydroxylated oxide surface orients the less polar acrylic portion of each ligand away from the particle surface essentially forming a hydrophobic coating. The presence of this coating should enhance the miscibility of the functionalized particles in nonpolar media by masking the highly polar hydroxylated oxide surface. To validate if the monomer coatings have had an impact on the stability and miscibility of nAl in common solvents we prepared a series of suspensions designed to compare the stability of the functionalized powders to the unfunctionalized nAl in common solvents and monomers. The suspensions were prepared by combining 0.030 g of the respective powders with 10 mL of solvent in a glass vial. The mixtures were then transferred to an ultrasonic bath for 60 seconds to suspend the particles. The solvents used for this study included water, toluene, ethanol, MMA, styrene and lauryl methacrylate (LMA). MMA, styrene and LMA were chosen as model monomers to represent mixtures that might be used to prepare a polymer nanocomposite from the functionalized nAl powders. Upon suspension, the vials were placed next to each other to compare their stability. This was done through careful observation of the time that was required for the particles to settle out of the suspensions. Images were acquired at various times during the settling process to document the visual appearance of the suspensions. In all of the suspensions studied the particles did eventually settle out of the suspension, although the time required for complete settling varied widely between the suspensions illustrating the differences in the chemical nature of coatings on the particles.

Suspensions prepared in toluene (Fig. 6) were clearly more stable for the functionalized powders than for neat nAl which began to settle immediately upon removal from the sonicator. Enhanced miscibility was also observed for suspensions prepared with the functionalized powders in both MMA and LMA with the exception of CEA-co-nAl which only partially suspended in both momoners. A similar trend was also observed for ethanol, with CEA-co-nAl demonstrating partial miscibility while nAl, due to its polar oxide surface, was completely miscible. Fairly stable suspensions were also observed in styrene for all samples, including the neat nAl powder. A summary of the suspension stabilities is presented in Table 4. A collection of the images acquired for suspensions can be found in the Electronic Supplemental Information (Fig. S4).

Table 4 Summary of particle suspensions in common solvents

Sample	Solvent					
	toluene	ethanol	water	MMA	styrene	LMA
nAl	settled	miscible	miscible	settled	miscible	partially
MPS- <i>co</i> -nAl	miscible	miscible	partially	miscible	miscible	miscible
CEA- <i>co</i> -nAl	miscible	settled	partially	partially	miscible	settled
PAM- <i>co</i> -nAl	miscible	miscible	miscible	miscible	miscible	miscible

**Fig. 6** Picture of toluene suspensions prepared with (left to right) nAl, MPS-*co*-nAl, CEA-*co*-nAl and PAM-*co*-nAl, respectively, after 1 minute.

The most intriguing observations obtained from this study came from the suspensions which were prepared in water. Although our primary focus was to alter the surface chemistry of nAl to promote compatibility within organic systems such as polymers and solvents, to aid in the preparation of high energy density nanocomposite materials, we also decided to study the effectiveness of these coatings in aqueous systems. Formulations of nAl and water (in the form of water or ice) have recently been demonstrated as effective solid rocket propellants.^{6,7} Generally speaking, nAl suspensions prepared in water are relatively unstable, as the particles oxidize over time, slowly consuming the metallic aluminum, yielding aluminum oxide and hydrogen as a gaseous bi-product. Our hypothesis is that the monomer coatings we have introduced might also provide a sufficient hydrophobic barrier which would limit diffusion of water to the particle surface thereby extending the lifetime of the particles in aqueous media. To test this theory we prepared suspensions of the functionalized powders in water and investigated their stability and resistance to oxidation in comparison to an aqueous suspension of neat nAl. As displayed in Fig 7a, stable suspensions were obtained for all of the powders in

water with the exception, again, of CEA-*co*-nAl which was partially miscible and settled out of the suspension.

The neat nAl powder easily suspended in water requiring minimal sonication; however, MPS-*co*-nAl significantly repelled the water required significant sonication to suspend. Even after sonication the MPS-*co*-nAl adhered to the sides of the glass vial. Only mild sonication was required to suspend PAM-*co*-nAl in water. After preparation all four suspensions were allowed to sit undisturbed. Although the particles eventually settled out from each of the suspensions during this period of time, oxidation occurred in the nAl, CEA-*co*-nAl and eventually MPS-*co*-nAl suspensions as was easily observed through color changes in the powders (Fig. 7b,c).

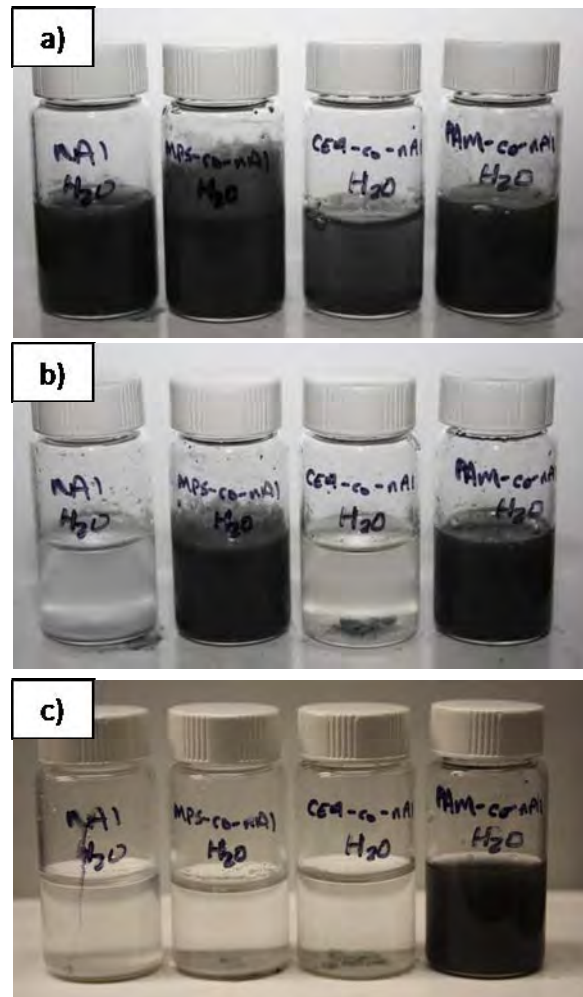


Fig. 7 (Left to right) nAl, MPS-*co*-nAl, CEA-*co*-nAl and PAM-*co*-nAl suspensions in water after a) 1 minute, b) 144 hours and c) 536 hours at room temperature.

Oxidation resulted in a transition from the original deep gray/black color to a lighter gray and finally to white. This was accompanied by the presence of bubbles in the solvent, presumably from the evolution of hydrogen gas. Noticeable oxidation of the neat nAl powder began after 32 hours of exposure to the water with complete oxidation occurring after 46 hours. The functionalized particles demonstrated far better resistance to oxidation when compared to the neat powder. MPS-*co*-nAl and PAM-*co*-nAl both displayed significant resistance to oxidation, at room temperatures, with the solutions retaining their original black color even after 144 hours exposure to water. As previously mentioned, CEA-*co*-nAl did eventually undergo oxidation during the 144 hour time frame; however, this occurred more gradually than in the neat powder and was not complete even after 144 hours, as can be seen by the gray aggregates of powder at the bottom of the vial in Fig 7b. Partial oxidation of MPS-*co*-nAl did eventually occur after *ca.* 350 hours of exposure to water, yet the PAM-*co*-nAl suspension still showed no signs of oxidation, retaining its original dark gray-black color, after more than 540 hours (22.5 days) of exposure at room temperature. These results confirm trends observed in a similar study which observed the stability of SAMs prepared with perfluorinated organosilanes, carboxylic acids, and phosphoric acids on bulk aluminum substrates in aqueous environments.¹⁸

In addition to the room temperature aqueous oxidation study we also investigated the integrity of the coatings when exposed to an elevated temperature of 75 °C to accelerate the rate of oxidation. It was not terribly surprising that trends which paralleled the room temperature study were also observed at elevated temperatures, however an increase in the rate of oxidation was observed. Gas evolution was observed in the MPS-*co*-nAl suspension after *ca.* 45 minutes, however, no visible color change was observed until 52 minutes and oxidation was complete after 58 minutes. Gas evolution in the nAl suspension began at *ca.* 52 minutes with noticeable oxidation occurring between 58-62 minutes. CEA-*co*-nAl began showing signs of oxidation after 66 minutes with complete oxidation occurring after 74 minutes. Heat was removed from the suspensions after 3 hours. The nAl, CEA-*co*-nAl and MPS-*co*-nAl suspensions had all demonstrated significant oxidation having turned mostly white in color. It is worth noting that the stability of the MPS coating was greatly affected by the elevated temperatures. Room temperature oxidation of the MPS-*co*-nAl did not occur until after 144 hours, lasting far longer than nAl and CEA-*co*-nAl, however, at 75 °C the MPS-*co*-nAl suspension was the first sample to oxidize, with oxidation occurring slightly before nAl. Surprisingly, the PAM-*co*-nAl suspension still displayed no visible signs of oxidation and retained its original color even after more than two hours at elevated temperatures. Images obtained from the accelerated oxidation study are presented in Fig. S5 located in the Electronic Supplemental Material section.

General discussion

Consideration of the collective data presented above strongly suggests that functionalization of nAl with acrylic monomers which contain reactive silane, carboxylic acid and phosphoric acid moieties does sufficiently alter the chemistry of the nAl surface. Not only does the addition of the monomers to the particles' surface promote their dispersion and miscibility in common nonpolar solvents such as toluene, but we have also shown the monomeric coatings are also capable of influencing the oxidation resistance of the particles in aqueous environments. For all monomers studied, functionalization occurs through chemical attachment of the monomer to the oxide surface, either through reaction (condensation) with the hydroxyls present on the passivated oxide surface or with the oxidized aluminum atoms within the oxide. Through careful investigation of the FTIR and XPS data we found that both MPS and PAM likely form covalent bonds to the oxide surface through reaction of the respective silane and phosphoric acid moieties with surface hydroxyls present on the oxide. The thermal stability of these coatings, under an inert atmosphere, also confirms that these coatings are likely anchored to the oxide through covalent bonds and are not merely physisorbed.

Interaction of CEA with the passivated oxidized surface of nAl appears to occur through the ionic interaction of the carboxylate, $-\text{COO}^-$, anion with oxidized aluminum (Al^{3+}) within the amorphous oxide. Additionally, it was clear from the TGA decomposition data for CEA-co-nAl that the monomer also undergoes thermally induced polymerization under the selected reaction conditions which leads to the presence of polymer on the particle surface. This is not observed in the case of MPS or PAM.

It is clear from the miscibility studies that the monomeric coatings clearly have an impact on the compatibility of nAl in organic solvents and polymeric systems which was the primary motivation for performing this work. Improving the miscibility of nAl increases the likelihood for incorporating these powders in nanocomposites and future high energy reactive materials. In addition to improving compatibility with organic systems, MPS and PAM monomer coatings also significantly reduces the oxidation of nAl when exposed to aqueous environments. Though this was not the initial intention of this study, improving the oxidation resistance of nAl in aqueous environments could potentially be critical enabler for emerging technologies such as nAl – water/ice based propellants^{6,7} or beneficial in providing a controlled time-release of hydrogen gas in nAl – water reactors.^{40,41}

Conclusions

We report the successful grafting of three acrylic monomers MPS, CEA and PAM to the amorphous oxide surface of nAl through reaction with the surface hydroxyls present at the particle surface or, in the case

of CEA, interaction with Al³⁺ at the particle surface. Through calculation of their individual grafting densities it was found that MPS reacts to form a near monolayer on the particle surface, while both CEA and PAM react to form multilayers. Additionally, we have shown that CEA also undergoes polymerization, even in the presence of an inhibitor, resulting a coating that consists of both monomer and polymer. Regardless of monomer, complete functionalization is achieved within 8 hours. The functionalized particles demonstrate enhanced miscibility with nonpolar organic solvents and acrylic monomers in comparison to the unfunctionalized nAl powder. Additionally, the PAM and MPS coatings are effective at inhibiting oxidation of nAl in aqueous environments for extended periods of time at room temperature while the PAM coating provides extended resistance to oxidation even at elevated temperatures. These findings could potentially have a strong impact for process of new high energy density composite materials.

Acknowledgements

The authors would like to thank Drs. C.E. Bunker, J.L. Jordan, C.M. Lindsay, K.A.S. Fernando and W.K. Lewis for useful discussions and assistance with data collection. Additionally, the authors would also like to acknowledge Mr. W.A. Houston and Mr. J.M. Scott for technical support. Funding for this work was made available by Air Force Research Laboratory, Materials and Manufacturing Directorate, from the Nanoscience and Technology STT Initiative in Nanoenergetics. Their support is gratefully acknowledged. This research was performed while the author (C.A. Crouse) held a National Research Council Post-doctoral Research Associateship.

References

- ¹ Dreizin, E.L. *Prog. Energy Comb. Sci.* **2009**, *35*, 141-167
- ² Levitas, V.I.; Asay, B.W.; Son, S.F.; Pantoja, M. *J. Appl. Phys.* **2007**, *101*, 083524
- ³ Sun, J.; Pantoja, M.L.; Simon, S.L. *Thermochim. Acta* **2006**, *444*, 117-127
- ⁴ Pantoja, M.L.; Granier, J.J. *Propellants Explos Pyrotech.* **2005**, *30*, 53-62
- ⁵ Brousseau, P.; Anderson, C.J. *Propellants Explos Pyrotech.* **2002**, *27*, 300-306
- ⁶ Ingenito, A.; Bruno, C. *J. Propul. Power* **2004**, *20*, 1056-1063

⁷ Risha, G.A.; Son, S.F.; Yetter, R.A.; Yang, V.; Tappan, B.C. *Proc. Combust. Inst.* **2007**, *31*, 2029-2036

⁸ Brege, J.J.; Hamilton, C.E.; Crouse, C.A.; Barron, A.R. *Nano Lett.* **2009**, *9*, 2239-2242

⁹ Jouet, R.J.; Warren, A.D.; Rosenburg, D.M.; Bellitto, V.J.; Park, K.; Zachariah, M.R. *Chem. Mater.* **2005**, *17*, 2987-2996

¹⁰ Gromov, A.A.; Forter-Barth, U.; Teipel, U. *Powder Techn.* **2006**, *164*, 111-115

¹¹ Kwon, Y-S.; Gromov, A.A.; Strokova, J.I. *Appl. Surf. Sci.* **2007**, *253*, 5558-5564

¹² Foley, T.J.; Johnson, C.E.; Higa, K.T. *Chem. Mater.* **2005**, *17*, 4086-4091

¹³ Meziani, M.J.; Bunker, C.E.; Lu, F.; Li, H.; Wang, W.; Guliants, E.A.; Quinn, R.A.; Sun, Y.-P. *ACS Appl. Mater. Interfaces* **2009**, *1*, 703-709

¹⁴ Crouse, C.A.; Shin, E.; Murray, P.T.; Spowart, J.E. *Mater. Lett.* **2010**, *64*, 271-274

¹⁵ Balazs, A.C.; Emerick, T.; Russell, T.P. *Science* **2006**, *314*, 1107-1110

¹⁶ Wefers, K.; Mirsa, C. *Oxides and hydroxides of Aluminum* **1988**, Alcoa Technical Paper No. 19, revised

¹⁷ Oberg, K.; Persson, P.; Shchukarev, A.; Eliasson, B. *Thin Solid Films* **2001**, *397*, 102-108

¹⁸ DeRose, J.A.; Hoque, E.; Bhushan, B.; Mathieu, H.J. *Surf. Sci.* **2008**, *602*, 1360-1367

¹⁹ Lim, M.S.; Feng, K.; Chen, X.; Wu, N.; Raman, A.; Nightingale, J.; Gawalt, E.S.; Korakakis, D.; Hornak, L.A.; Tiperman, A.T. *Langmuir* **2007**, *23*, 2444-2452

²⁰ Karaman, M.E.; Antelmi, D.A.; Pashley, R.M. *Colloids Surf., A* **2001**, *182*, 285-298

²¹ Taylor, C.E.; Schwartz, D.K. *Langmuir* **2003**, *19*, 2665-2672

²² Abel, M.L.; Watts, J.F.; Digby, R.P. *Int. J. Adhes. Adhes.* **1998**, *18*, 179-192

²³ Kallury, K.M.R.; Cheung, M.; Ghaemmaghami, V.; Krull, U.J.; Thompson, M. *Colloids Surf.* **1992**, *63*, 1-9

²⁴ Goldstein, C.S.; Weiss, K.D.; Drago, R.S. *J. Am. Chem. Soc.* **1987**, *109*, 758-761

²⁵ Liakos, I.L.; McAlpine, E.; Chen, X.; Newman, R.; Alexander, M. *Appl. Surf. Sci.* **2008**, *255*, 3276-3282

²⁶ Spori, D.M.; Venkataraman, N.V.; Tosatti, S.G.P.; Durmaz, F.; Spencer, N.D.; Zurcher, S. *Langmuir* **2007**, *23*, 8053-8060

²⁷ Guo, Z.; Pereira, T.; Choi, O.; Wang, Y.; Hahn, H.T. *J. Mater. Chem.* **2006**, *16*, 2800-2808

²⁸ Ash, B.J.; Rogers, D.F.; Weigand, C.J.; Schadler, L.S.; Siegel, R.W.; Benicewicz, B.C.; Apple, T. *Polym. Composite* **2002**, *23*, 1014-1025

²⁹ Liu, H.; Ye, H.; Zhang, Y. *Colloid Surf., A* **2008**, *315*, 1-6

³⁰ Liu, H.; Ye, H.; Zhang, Y.; Tang, X. *Dyes Pigm.* **2008**, *79*, 236-241

³¹ Manufacturer reported average particle size (APS) and specific surface areas (SSA). a) Alfa Aesar, aluminum powder (Lot # C11T058), 18 nm APS, SSA: not reported; b) Nanostructured & Amorphous Materials, Inc., aluminum nanopowder (Lot#0136-010808), 18 nm APS, SSA: 40-60 m²/g; c) American Elements, aluminum metal nanopowder (Lot#1031396379-818), 10-30 nm APS, SSA: 20-40 m²/g.

³² Wasserman, S.R.; Whitesides, G.M.; Tidswell, I.M.; Ocko, B.M.; Pershan, P.S.; Axe, J.D. *J. Am. Chem. Soc.* **1989**, *111*, 5852-5861

³³ Adiga, S.P.; Zapol, P.; Curtis, L.A. *J. Phys. Chem. C* **2004**, *111*, 7422-7429

³⁴ Hu, Y.-H.; Chen, C.-Y. *Poly. Degrad. Stab.* **2003**, *82*, 81-88

³⁵ Holland, B.J.; Hay, J.N. *Polym. Degrad. Stab.* **2002**, *77*, 435-439

³⁶ Fyfe, C.A.; McKinnon, M.S. *Macromolecules* **1986**, *19*, 1909-1912

³⁷ Mauere, J.J.; Eustace, D.J.; Ratcliffe, C.T. *Macromolecules* **1987**, *20*, 196-202

³⁸ Shek, C.H.; Lai, J.K.L.; Gu, T.S.; Lin, G.M. *Nanostruct. Mater.* **1997**, *8*, 605-610

³⁹ Sah, A.; Castricum, H.L.; Bliek, A.; Blank, D.H.A.; ten Elshof, J.E. *J. Membrane Sci.* **2004**, *243*, 125-132

⁴⁰ Martinez, S.S.; Sanchez, L.A.; Gallego, A.A.A.; Sebastian, P.J. *Int. J. Hydrogen Energ.* **2007**, *32*, 3159-3162

⁴¹ Soler, L.; Macanas, J.; Munoz, M.; Casado, J. *J. Power Sources* **2007**, *169*, 144-149

Electronic Supporting Information

Influencing solvent miscibility and aqueous stability of oxide passivated aluminum nanoparticles through surface functionalization with acrylic monomers

Christopher A. Crouse,^{a,b*} Christian J. Pierce^a and Jonathan E. Spowart^a

^a Air Force Research Laboratory, Materials and Manufacturing Directorate, Wright-Patterson Air Force Base, OH 45433, USA

^b UES, Inc., Dayton, OH 45432, USA

*Corresponding author: christopher.crouse@wpafb.af.mil

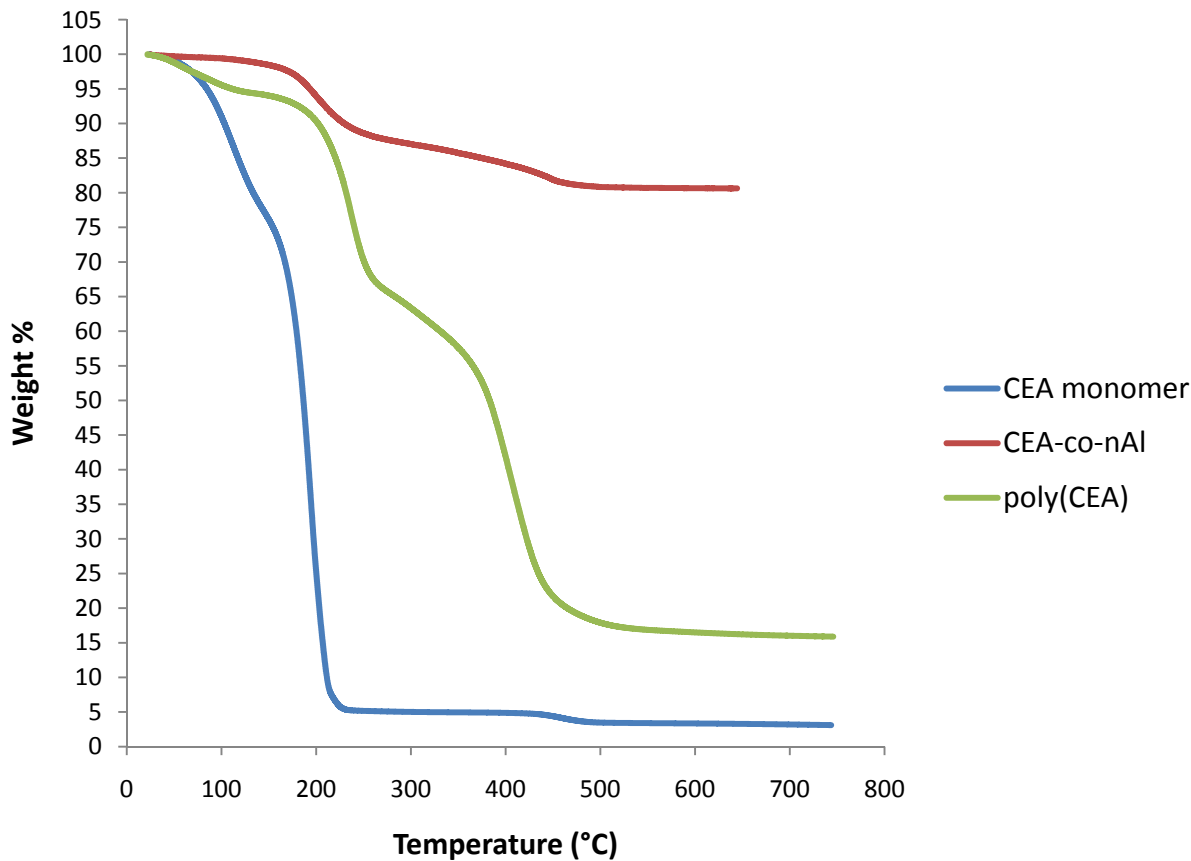


Fig. S1 TGA overlay displaying the decomposition of CEA monomer (blue), CEA-co-nAl (red) and poly(CEA) (green).

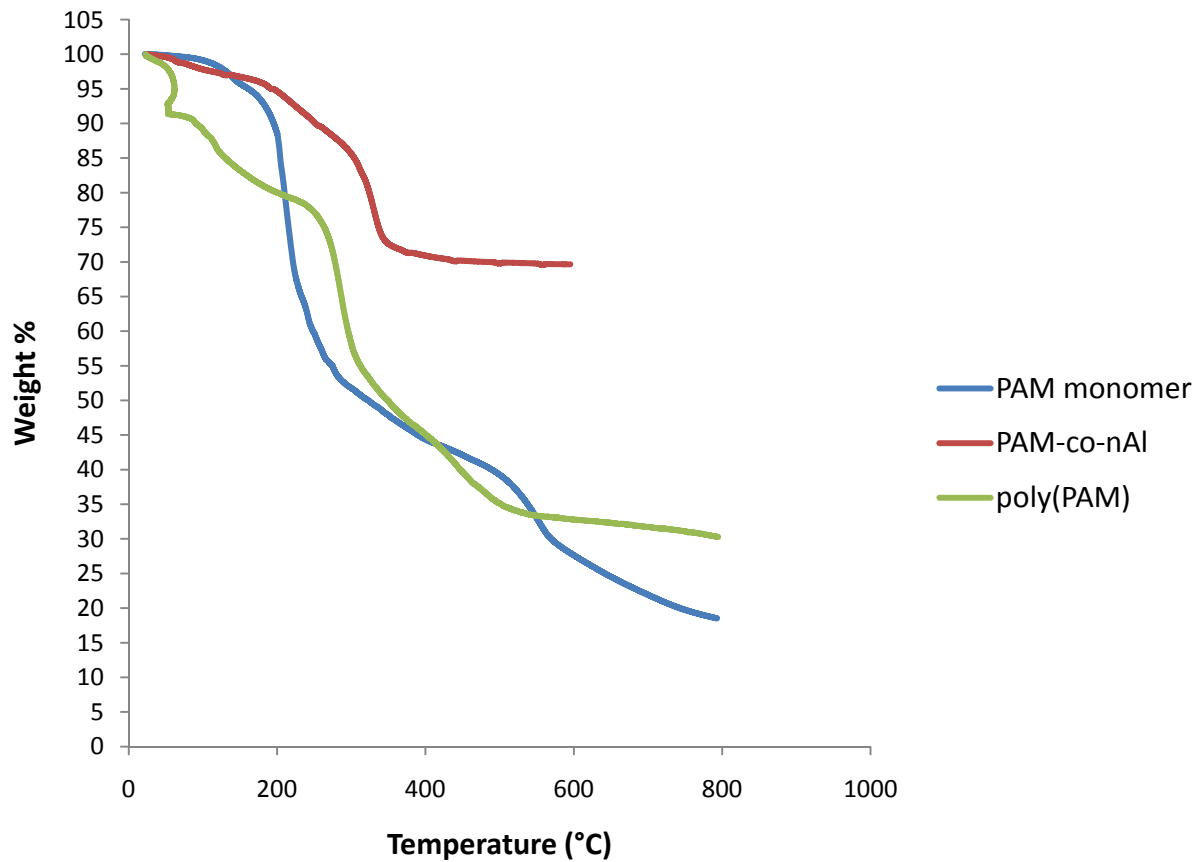


Fig. S2 TGA overlay displaying the decomposition of PAM monomer (blue), PAM-*co*-nAl (red) and poly(PAM) (green).

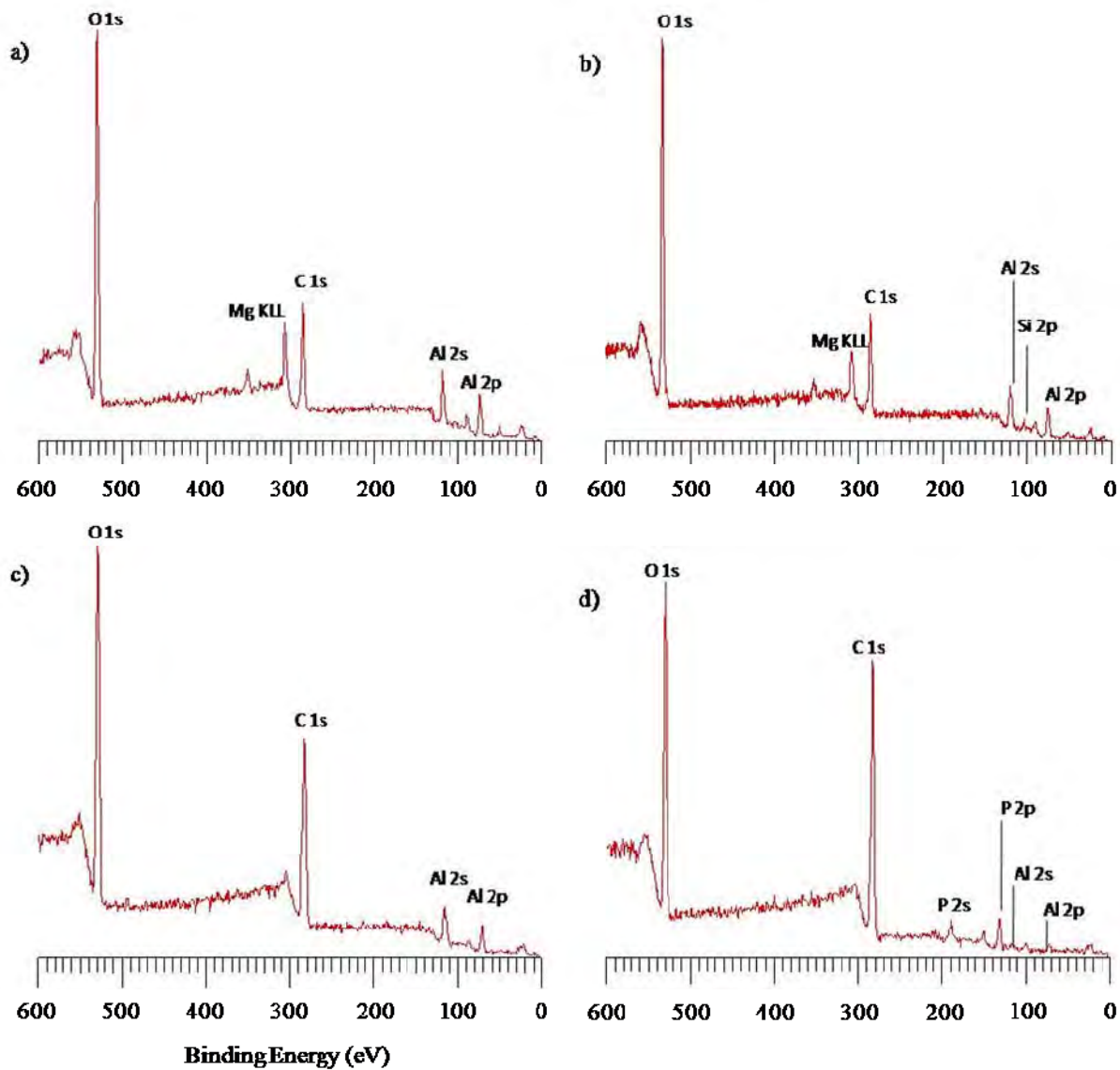


Fig.S3 XPS survey spectra for a) nAl, b) MPS-*co*-nAl, c) CEA-*co*-nAl and d) PAM-*co*-nAl.

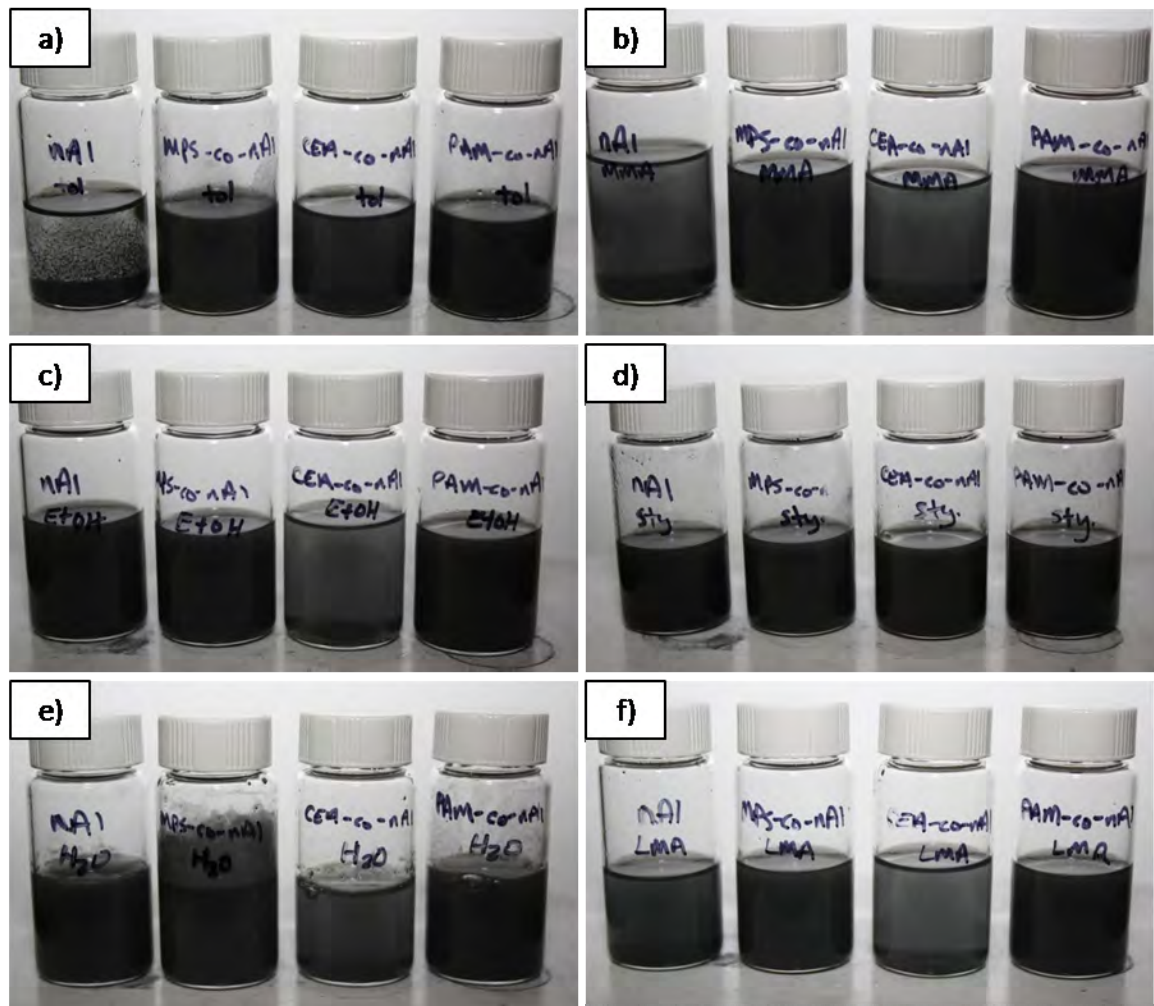


Fig. S4 Suspension of (Left to right) nAl, MPS-co-nAl, CEA-co-nAl, PAM-co-nAl in a) toluene, b) methyl methacrylate, c) ethanol, d) styrene, e) water and f) lauryl methacrylate after 1 minute.

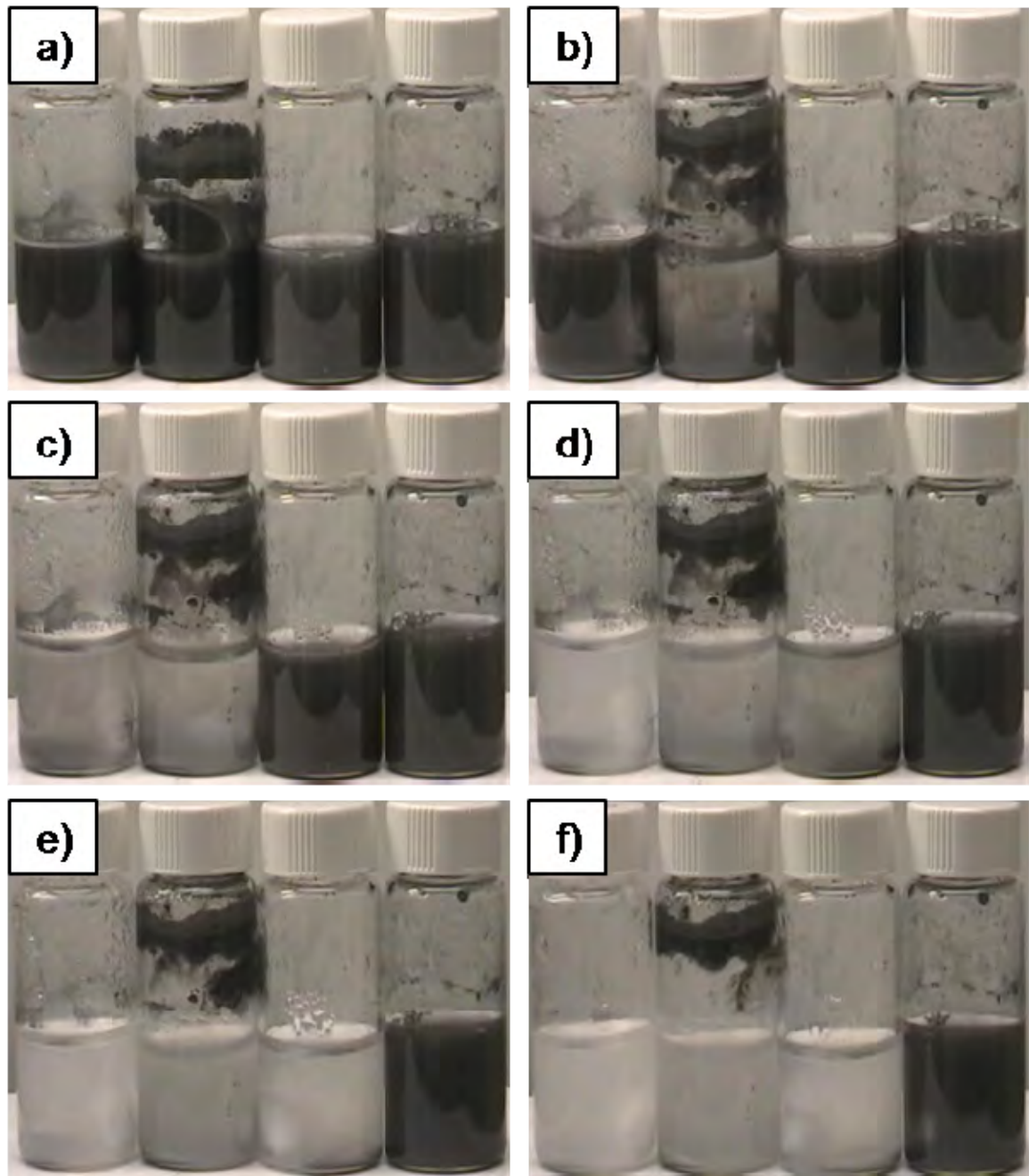


Fig. S5 Images from the aqueous oxidation of (left to right) nAl, MPS-co-nAl, CEA-co-nAl, PAM-co-nAl at 75 °C after a) 45 minutes, b) 56 minutes, c) 62 minutes, d) 70 minutes, e) 80 minutes, and f) 135 minutes.